Fast Calculation of Energy and Mass preserving solutions of Schrödinger–Poisson systems on unbounded domains

Matthias Ehrhardt *,[1] and Andrea Zisowsky [1]

Institut für Mathematik, Technische Universität Berlin, Strasse des 17. Juni 136, D–10623 Berlin, Germany

Abstract

This paper deals with the numerical solution of the time–dependent Schrödinger–Poisson system in the spherically symmetric case. Since the problem is posed on an unbounded domain one has to introduce artificial boundary conditions to confine the computational domain. The main topic of this work is the construction of a so–called discrete transparent boundary condition (TBC) for a Crank–Nicolson-type predictor–corrector scheme for solving the Schrödinger–Poisson system. This scheme has the property of mass and energy conservation exactly on the discrete level. We propose different strategies for the discrete TBC and present an efficient implementation. Finally, a numerical example illustrate the findings and shows the comparison results between the different approaches.

Key words: Schrödinger–Poisson system, Schrödinger equation, finite differences, discrete transparent boundary conditions, difference equation, Newton potential
PACS: 02.70.Bf, 31.15.Fx, 95.30.Cq

* Corresponding author.
Email addresses: ehrhardt@math.tu-berlin.de (Matthias Ehrhardt), zisowsky@math.tu-berlin.de (Andrea Zisowsky).
URLs: http://www.math.tu-berlin.de/~ehrhardt/ (Matthias Ehrhardt), http://www.math.tu-berlin.de/~zisowsky/ (Andrea Zisowsky).
[1] Supported by the DFG Research Center "Mathematics for key technologies" (FZT 86) in Berlin.

1 Introduction

In many applications in quantum mechanics one wants to calculate the evolution of an ensemble of particles over long time. This computations include the solution of the single particle Schrödinger equation obtained from a mean field approximation using Coulomb potentials [16]. The transient Schrödinger–Poisson problem describes the time evolution of the wave function ψ under the force of the self–consistent potential V caused by the charged electrons. It is an appropriate model for semiconductor heterostructures (cf. [16] and the references therein). We note that Schrödinger–Poisson systems appear in different applications, e.g. electron confinement in quantum nanostructures [14] or as a description for the helium ground state in astrophysical applications [19].

1.1 The Schrödinger–Poisson system. The transient *Schrödinger–Poisson system* (SPS) associated with a single particle system in vacuum reads for the complex–valued wave function $\psi(x,t)$ and the electrostatic potential $V(x,t)$:

$$i\hbar\partial_t\psi = -\frac{\hbar^2}{2m}\Delta_x\psi + V\psi, \qquad x\in\mathbb{R}^3, \quad t>0, \tag{1a}$$

$$\Delta_x V = -\gamma\, n, \qquad x\in\mathbb{R}^3, \quad t>0, \tag{1b}$$

where $n=|\psi(x,t)|^2$ denotes the expected particle density for a pure quantum state and $\gamma>0$ (repulsive case) or $\gamma<0$ (attractive case) depending on the considered type of Coulomb force. Here $\hbar$ denotes the Planck constant and m is the particle mass. Throughout this paper we are interested in the attractive case where the Schrödinger–Poisson system describes the time evolution of an electron in a polar crystal (a polaron) under the assumption that the phonon cloud or lattice vibrations behave classically. However, our results also hold in the repulsive case. Equations (1) are supplied with some initial data $\psi(x,0)=\psi^I(x)$ and the decay conditions

$$\lim_{|x|\to\infty}\psi(x,t)=0, \qquad \lim_{|x|\to\infty}V(x,t)=0.$$

The self–consistent potential V created by the charged electrons is obtained as solution to (1b), and can be written explicitly as

$$V(x,t)=\frac{\gamma}{4\pi}\int_{\mathbb{R}^3}\frac{n(x',t)}{|x-x'|}\,dx'. \tag{2}$$

We remark that the existence and uniqueness of solutions to the Schrödinger–Poisson system were analyzed in [7], [12]. Recently, a transient Schrödinger–Poisson system in dimension 2 or 3 with transparent boundaries was studied [5] (the one–dimensional case was already treated in [4]). Finally, we note

that the Schrödinger–Poisson system is sometimes called *Schrödinger–Newton equations*; the stationary spherical–symmetric case was investigated numerically in [18] and analytically in [24].

1.2 The spherically symmetric Schrödinger–Poisson system. Since we want to keep the numerical effort to a minimum we only consider the case of a spherically symmetric *initial condition*: $\psi(x,0) = \psi^I(r)$. It can be shown that $\psi(x,t)$ is invariant under rotations and therefore a radial function at any time. For convenience we introduce the *reduced wave function* $u(r,t)$ by

$$\psi(x,t) = \frac{1}{\sqrt{4\pi}} \frac{u(r,t)}{r}, \tag{3}$$

and define the *effective charge* $\phi(r,t) = rV(x,t)$ which becomes using (2)

$$\phi(r,t) = \frac{\gamma}{4\pi} \left(\int_0^r |u(r',t)|^2 \, dr' + \int_r^\infty \frac{r}{r'} |u(r',t)|^2 \, dr' \right). \tag{4}$$

Differentiating (4) twice with respect to the radial coordinate r, the *SPS* reduces then to

$$i\hbar \partial_t u = -\frac{\hbar^2}{2m} \partial_r^2 u + \frac{\phi}{r} u, \qquad r > 0, \quad t > 0, \tag{5a}$$

$$\partial_r^2 \phi = -\frac{\gamma}{4\pi} \frac{|u|^2}{r}, \qquad r > 0, \quad t > 0, \tag{5b}$$

together with the *homogeneous Dirichlet conditions at the origin*

$$u(0,t) = 0, \qquad \phi(0,t) = 0,$$

and the *decay conditions*

$$\lim_{r\to\infty} u(r,t) = 0, \qquad \lim_{r\to\infty} \phi(r,t) = \frac{\gamma}{4\pi}.$$

1.3 The conserved Quantities. The practically most important conserved quantities usually are the *mass of particles* and the *total energy*. The mass of particles is simply the L^2–norm of u and therefore we can choose as *normalization condition*

$$\int_0^\infty |u(r,t)|^2 \, dr = 1, \quad t > 0. \tag{6}$$

The *conserved total energy* is given by

$$E(t) = E_{\mathrm{KIN}}(t) + E_{\mathrm{INT}}(t) + E_{\mathrm{POT}}(t), \quad t > 0, \tag{7}$$

where the kinetic, interaction and potential energies are

$$E_{\mathrm{KIN}}(t) = \frac{\hbar^2}{2m} \int_0^\infty |\partial_r u(r,t)|^2 \, dr, \quad t > 0, \tag{8a}$$

$$E_{\mathrm{INT}}(t) = \int_0^\infty \frac{\phi(r,t)}{r} \, |u(r,t)|^2 \, dr, \quad t > 0, \tag{8b}$$

$$E_{\mathrm{POT}}(t) = \frac{2\pi}{\gamma} \int_0^\infty \partial_r \phi(r,t)^2 \, dr, \quad t > 0. \tag{8c}$$

When solving the SPS numerically it is desirable that the discrete L^2–norm (mass of particles) and the discrete total energy are preserved *exactly* by the numerical scheme because discretization errors in the conservation laws accumulate. While it is easy to conserve the discrete L^2–norm (yielding an unitary evolution) it turns out that it is not so trivial to preserve simultaneously the *total energy*

$$E(t) = \frac{\hbar^2}{2m} \int_0^\infty |\partial_r u(r,t)|^2 \, dr + \frac{1}{2} \int_0^\infty \frac{\phi(r,t)}{r} \, |u(r,t)|^2 \, dr, \quad t > 0. \tag{9}$$

In this paper we consider the second order *predictor–corrector scheme of Ringhofer and Soler* [20] where the discretization is based on the Crank–Nicolson scheme. The conservation of mass and energy is achieved by introducing a *phase modulation* in the corrector step.

Remark 1 *We remark that one can get an arbitrarily high (even) order mass–conservative scheme for the Schrödinger equation by using the diagonal Padé approximations to the exponential [3]. The Crank–Nicolson scheme corresponds to second order, and the fourth order is known in the ODE literature as Hammer and Hollingsworth method [11].*

The outline of the paper is as follows. First we review briefly in §2 the approach of Ringhofer and Soler since their presentation in [20] is rather abstract and details concerning a concrete implementation, e.g. appropriate boundary conditions, are omitted. Afterwards in §3 we construct a so–called *discrete transparent boundary condition* (DTBC) for a Schrödinger equation with a Newton–type potential term, and discuss different approaches to obtain discrete asymptotic solutions. We present in §4 an efficient implementation by the *sum–of–exponentials ansatz* that reduces the computational effort for implementing the DTBC significantly. Finally, we illustrate the results with a numerical example comparing the different proposed versions of the DTBC.

2 The Numerical Schemes

In this section we first review the *nonlinear Crank–Nicolson scheme* from [20] and show its conservation properties. Afterwards we turn to the *linear predictor–corrector scheme* proposed by Ringhofer and Soler and analyze its conservation properties, too. For simplicity of the presentation we will only

deal with uniform grids: (for a nonuniform time discretization and a general spatial discretization cf. [20]):

$$u_j^{(n)} \sim u(r_j, t_n), \quad \phi_j^{(n)} \sim \phi(r_j, t_n), \qquad r_j = j\Delta r, \quad t_n = n\Delta t,$$

with $0 \le j \le J$, $n \ge 0$.

2.1 The nonlinear Crank–Nicolson scheme. The *discretized SPS* reads

$$i\hbar D_t^+ u_j^{(n)} = -\frac{\hbar^2}{2m} D_r^2 u_j^{(n+\frac{1}{2})} + \frac{\phi_j^{(n+\frac{1}{2})}}{r_j} u_j^{(n+\frac{1}{2})}, \quad j \ge 1, \tag{10a}$$

$$D_r^2 \phi_j^{(n+1)} = -\frac{\gamma}{4\pi} \frac{\left|u_j^{(n+1)}\right|^2}{r_j}, \quad j \ge 1, \tag{10b}$$

together with the discrete boundary conditions

$$u_0^{(n)} = 0, \qquad \lim_{j\to\infty} u_j^{(n)} = 0, \qquad \phi_0^{(n)} = 0, \qquad \phi_J^{(n)} = \frac{\gamma}{4\pi}. \tag{10c}$$

A realization of the decay condition for $u_j^{(n)}$ in the form of a (discrete) transparent boundary condition will be the topic of §3. In (10) we have used the standard abbreviations for the forward, and second order difference quotient:

$$D_t^+ u_j^{(n)} = \frac{u_j^{(n+1)} - u_j^{(n)}}{\Delta t}, \quad D_r^2 u_j^{(n)} = \frac{u_{j+1}^{(n)} - 2u_j^{(n)} + u_{j-1}^{(n)}}{(\Delta r)^2},$$

and the time averaging $u_j^{(n+\frac{1}{2})} = (u_j^{(n+1)} + u_j^{(n)})/2$.

Discrete conservation properties of the nonlinear scheme. First we want to show the discrete conservation of the *mass* (cf. (6))

$$\|u^{(n)}\|_2^2 := \Delta r \sum_{j=0}^{\infty} \left|u_j^{(n)}\right|^2. \tag{11}$$

Here and in the sequel we will need a simple identity (*"discrete product rule"*)

$$D_t^+(u^{(n)} w^{(n)}) = u^{(n+\frac{1}{2})} D_t^+(w^{(n)}) + w^{(n+\frac{1}{2})} D_t^+(u^{(n)}), \tag{12}$$

i.e. with $w^{(n)} = \bar{u}^{(n)}$ we get

$$D_t^+ \left|u^{(n)}\right|^2 = 2\,\mathrm{Re}\{\bar{u}^{(n+\frac{1}{2})} D_t^+ u^{(n)}\}. \tag{13}$$

To derive the *discrete mass conservation property* we consider the discretized SPS (10) on the finite domain $1 \le j \le J-1$ and multiply (10a) with $-i\bar{u}_j^{(n+\frac{1}{2})}$:

$$\hbar \bar{u}_j^{(n+\frac{1}{2})} D_t^+ u_j^{(n)} = \frac{i\hbar^2}{2m} \bar{u}_j^{(n+\frac{1}{2})} D_r^2 u_j^{(n+\frac{1}{2})} - i\frac{\phi_j^{(n+\frac{1}{2})}}{r_j} \left|u_j^{(n+\frac{1}{2})}\right|^2. \tag{14}$$

Summing up (14) for $1 \le j \le J-1$ gives with summation by parts

$$\sum_{j=1}^{J-1} \bar{u}_j^{(n+\frac{1}{2})} D_t^+ u_j^{(n)} = -\frac{i\hbar}{2m} \sum_{j=0}^{J-1} \left| D_r^+ u_j^{(n+\frac{1}{2})} \right|^2 - \frac{i}{\hbar} \sum_{j=1}^{J-1} \frac{\phi_j^{(n+\frac{1}{2})}}{r_j} \left| u_j^{(n+\frac{1}{2})} \right|^2 + \frac{i\hbar}{2m\Delta r} \Big(\bar{u}_J^{(n+\frac{1}{2})} D_r^- u_J^{(n+\frac{1}{2})} - \bar{u}_0^{(n+\frac{1}{2})} D_r^+ u_0^{(n+\frac{1}{2})} \Big). \tag{15}$$

Taking the real part using (13) and the boundary condition at $j = 0$ yields:

$$D_t^+ \Delta r \sum_{j=0}^{J-1} \left| u_j^{(n)} \right|^2 = -\frac{\hbar}{m} \operatorname{Im} \Big\{ \bar{u}_J^{(n+\frac{1}{2})} D_r^- u_J^{(n+\frac{1}{2})} \Big\}, \tag{16}$$

i.e. for $J \to \infty$ the conservation of the mass.

Similarly one can derive the conservation of the *discrete total energy* $E^{(n)}$ (cf. (9)) which is defined at time step n by

$$E^{(n)} = \frac{\hbar^2 \Delta r}{2m} \sum_{j=0}^{\infty} \left| D_r^+ u_j^{(n)} \right|^2 + \frac{\Delta r}{2} \sum_{j=1}^{\infty} \frac{\phi_j^{(n)}}{r_j} \left| u_j^{(n)} \right|^2, \quad n \ge 0. \tag{17}$$

Multiplying (10a) with $-D_t^+ \bar{u}_j^{(n)}$ one gets

$$-i\hbar \left| D_t^+ u_j^{(n)} \right|^2 = \frac{\hbar^2}{2m} (D_t^+ \bar{u}_j^{(n)}) D_r^2 u_j^{(n+\frac{1}{2})} - \frac{\phi_j^{(n+\frac{1}{2})}}{r_j} u_j^{(n+\frac{1}{2})} D_t^+ \bar{u}_j^{(n)}.$$

Summing it up for the finite domain $1 \le j \le J-1$ gives

$$-i\hbar \sum_{j=1}^{J-1} \left| D_t^+ u_j^{(n)} \right|^2 = -\frac{\hbar^2}{2m} \sum_{j=1}^{J-1} (D_t^+ D_r^+ \bar{u}_j^{(n)}) D_r^+ u_j^{(n+\frac{1}{2})} - \sum_{j=1}^{J-1} \frac{\phi_j^{(n+\frac{1}{2})}}{r_j} u_j^{(n+\frac{1}{2})} D_t^+ \bar{u}_j^{(n)} + \frac{\hbar^2}{2m\Delta r} \Big((D_t^+ \bar{u}_J^{(n)}) D_r^- u_J^{(n+\frac{1}{2})} - (D_t^+ \bar{u}_0^{(n)}) D_r^+ u_0^{(n+\frac{1}{2})} \Big),$$

and taking the real part using again (13) and the boundary condition at $j = 0$:

$$\frac{\hbar^2}{2m} D_t^+ \sum_{j=0}^{J-1} \left| D_r^+ u_j^{(n)} \right|^2 + \sum_{j=1}^{J-1} \frac{\phi_j^{(n+\frac{1}{2})}}{r_j} D_t^+ \left| u_j^{(n)} \right|^2 = \frac{\hbar^2}{m\Delta r} \operatorname{Re} \Big\{ (D_t^+ \bar{u}_J^{(n)}) D_r^- u_J^{(n+\frac{1}{2})} \Big\}. \tag{18}$$

Using (10b), the second term of (18) can be written in the following way

$$\sum_{j=1}^{J-1} \frac{\phi_j^{(n+\frac{1}{2})}}{r_j} D_t^+ \left| u_j^{(n)} \right|^2 = -\frac{4\pi}{\gamma} \sum_{j=1}^{J-1} \phi_j^{(n+\frac{1}{2})} D_t^+ D_r^2 \phi_j^{(n)} = \frac{2\pi}{\gamma} D_t^+ \sum_{j=0}^{J-1} (D_r^+ \phi_j^{(n)})^2 - \frac{4\pi}{\gamma \Delta r} \phi_J^{(n+\frac{1}{2})} D_t^+ D_r^- \phi_J^{(n)}.$$

Now summation by parts yields

$$\begin{aligned}\sum_{j=1}^{J-1}\frac{\phi_j^{(n+\frac12)}}{r_j}D_t^+\left|u_j^{(n)}\right|^2 &= -\frac{2\pi}{\gamma}D_t^+\sum_{j=1}^{J-1}\phi_j^{(n)}D_r^2\phi_j^{(n)} - \frac{4\pi}{\gamma\Delta r}\phi_J^{(n+\frac12)}D_t^+D_r^-\phi_J^{(n)}\\ &\quad+\frac{2\pi}{\gamma\Delta r}D_t^+\Big(\phi_J^{(n)}D_r^-\phi_J^{(n)}-\phi_0^{(n)}D_r^+\phi_0^{(n)}\Big)\\ &= \frac{2\pi}{\gamma\Delta r}D_t^+(\phi_J^{(n)}D_r^-\phi_J^{(n)}) - \frac{4\pi}{\gamma\Delta r}\phi_J^{(n+\frac12)}D_t^+D_r^-\phi_J^{(n)}\\ &\quad+\frac12 D_t^+\sum_{j=1}^{J-1}\frac{\phi_j^{(n)}}{r_j}\left|u_j^{(n)}\right|^2\\ &= -\frac{2\pi}{\gamma\Delta r}\Big(\phi_J^{(n+\frac12)}D_t^+D_r^-\phi_J^{(n)}-(D_r^-\phi_J^{(n+\frac12)})D_t^+\phi_J^{(n)}\Big)\\ &\quad+\frac12 D_t^+\sum_{j=1}^{J-1}\frac{\phi_j^{(n)}}{r_j}\left|u_j^{(n)}\right|^2,\end{aligned}$$

i.e. (18) reads now

$$\begin{aligned}&D_t^+\left[\frac{\hbar^2\Delta r}{2m}\sum_{j=0}^{J-1}\left|D_r^+u_j^{(n)}\right|^2+\frac{\Delta r}{2}\sum_{j=1}^{J-1}\frac{\phi_j^{(n)}}{r_j}\left|u_j^{(n)}\right|^2\right]\\ &=\frac{2\pi}{\gamma}\Big(\phi_J^{(n+\frac12)}D_t^+D_r^-\phi_J^{(n)}-(D_r^-\phi_J^{(n+\frac12)})D_t^+\phi_J^{(n)}\Big)+\frac{\hbar^2}{m}\operatorname{Re}\Big\{(D_t^+\bar u_J^{(n)})D_r^-u_J^{(n+\frac12)}\Big\}.\end{aligned}\tag{19}$$

Letting $J\to\infty$ the boundary terms vanish and we obtain the *discrete energy conservation*: $D_t^+E^{(n)}=0$.

2.2 The Predictor–Corrector Scheme. We now proceed to present the predictor–corrector scheme approximating the nonlinear Crank–Nicolson scheme (10). It only requires the solution of linear equations at each step and is of the same order. One step of the predictor–corrector scheme will be of the form

$$(u_j^{(n)},\phi_j^{(n)})\to u_j^{(n,1)}\to\phi_j^{(n,1)}\to u_j^{(n,2)}\to\phi_j^{(n,2)}\to(u_j^{(n+1)},\phi_j^{(n+1)}),$$

where $u_j^{(n,1)}$, $\phi_j^{(n,1)}$, $u_j^{(n,2)}$, $\phi_j^{(n,2)}$ denote some intermediate values. For brevity we define the *difference operators* $D_{t,k}^+u_j^{(n)}=(u_j^{(n,k)}-u_j^{(n)})/\Delta t$, and the *time averaging* $S_{t,k}u_j^{(n)}=(u_j^{(n,k)}+u_j^{(n)})/2$, $k=1,2$.

Given $u_j^{(n)}$, the *predictor step* to compute $u_j^{(n,1)}$, $\phi_j^{(n,1)}$ is then defined as

$$i\hbar D_{t,1}^+ u_j^{(n)} = -\frac{\hbar^2}{2m} D_r^2 S_{t,1} u_j^{(n)} + \frac{\phi_j^{(n)}}{r_j} S_{t,1} u_j^{(n)}, \quad j \geq 1, \tag{20a}$$

$$D_r^2 \phi_j^{(n,1)} = -\frac{\gamma}{4\pi} \frac{\left|u_j^{(n,1)}\right|^2}{r_j}, \quad j \geq 1. \tag{20b}$$

Note that this represents two decoupled linear equations for $u_j^{(n,1)}$ and $\phi_j^{(n,1)}$, since the term $\phi_j^{(n+\frac{1}{2})}$ in (10a) has been replaced by $\phi_j^{(n)}$ in (20a).

The standard *corrector step* for determining $u_j^{(n,2)}$, $\phi_j^{(n,2)}$ is given by

$$i\hbar D_{t,2}^+ u_j^{(n)} = -\frac{\hbar^2}{2m} D_r^2 S_{t,2} u_j^{(n)} + \frac{S_{t,1}\phi_j^{(n)}}{r_j} S_{t,2} u_j^{(n)}, \quad j \geq 1, \tag{21a}$$

$$D_r^2 \phi_j^{(n,2)} = -\frac{\gamma}{4\pi} \frac{\left|u_j^{(n,2)}\right|^2}{r_j}, \quad j \geq 1. \tag{21b}$$

Again, this represents two decoupled linear systems for $u_j^{(n,2)}$, $\phi_j^{(n,2)}$. It is easily verified that the scheme (20)–(21) is second order consistent in time.

The conservation properties of the predictor–corrector scheme. In the following we want to study the conservation properties of the predictor–corrector scheme (20)–(21) on the domain $j \geq 1$. Note that an identity analogous to (12) holds: $D_{t,k}^+(u^{(n)}w^{(n)}) = S_{t,k}u^{(n)} D_{t,k}^+ w^{(n)} + S_{t,k} w^{(n)} D_{t,k}^+ u^{(n)}$, $k = 1, 2$. As before, the *discrete mass conservation* is verified by computing as in (14): multiplying (21a) with $-iS_{t,2}\bar{u}_j^{(n)}$, summing for $1 \leq j \leq J-1$ and taking the real part yields (as an analogy to (16)):

$$D_{t,2}^+ \Delta r \sum_{j=1}^{J-1} \left|u_j^{(n)}\right|^2 = -\frac{\hbar}{m} \operatorname{Im}\Big\{(S_{t,2}\bar{u}_J^{(n)}) D_r^- S_{t,2} u_J^{(n)}\Big\}. \tag{22}$$

Thus (letting $J \to \infty$), this predictor–corrector approach preserves mass.

To investigate the *energy conservation* properties of (20)–(21) we multiply (21a) by $-D_{t,2}^+ \bar{u}_j^{(n)}$ and obtain

$$\frac{\hbar^2}{2m} D_{t,2}^+ \sum_{j=0}^{J-1} \left|D_r^+ u_j^{(n)}\right|^2 + \sum_{j=1}^{J-1} \frac{S_{t,1}\phi_j^{(n)}}{r_j} D_{t,2}^+ \left|u_j^{(n)}\right|^2 = \frac{\hbar^2}{m\Delta r} \operatorname{Re}\Big\{(D_{t,2}^+ \bar{u}_J^{(n)}) D_r^- S_{t,2} u_J^{(n)}\Big\}. \tag{23}$$

In order to get an equation analogue to (18) we can write this as a correction to the nonlinear Crank–Nicolson scheme, i.e. we use $S_{t,1}\phi_j^{(n)} = S_{t,2}\phi_j^{(n)} - (\phi_j^{(n,2)} -$

$\phi_j^{(n,1)})/2$ in (23):

$$\frac{\hbar^2}{2m} D_{t,2}^+ \sum_{j=0}^{J-1} \left| D_r^+ u_j^{(n)} \right|^2 + \sum_{j=1}^{J-1} \frac{S_{t,2}\phi_j^{(n)}}{r_j} D_{t,2}^+ \left| u_j^{(n)} \right|^2 = \frac{1}{2} \sum_{j=1}^{J-1} \frac{\phi_j^{(n,2)} - \phi_j^{(n,1)}}{r_j} D_{t,2}^+ \left| u_j^{(n)} \right|^2 + \frac{\hbar^2}{m\Delta r} \operatorname{Re}\Big\{ (D_{t,2}^+ \bar{u}_J^{(n)}) D_r^- S_{t,2} u_J^{(n)} \Big\}. \tag{24}$$

2.3 The Modulation Strategy. Comparing (24) with (18) one notices that the predictor–corrector approximation to the Crank–Nicolson scheme preserves mass, but exhibits a spurious gain / loss of the total energy which is of order Δt^3 at each time step. Ringhofer and Soler remedied this situation by *modulating the phase* of the second stage $u_j^{(n,2)}$ of the scheme by setting

$$u_j^{(n+1)} = u_j^{(n,2)} \exp(i\Delta t^3 \omega g_j), \qquad \phi_j^{(n+1)} = \phi_j^{(n,2)}, \quad j \geq 1, \tag{25}$$

where ω is a real parameter and $g_j = g(r_j)$ denotes an appropriate chosen real valued function bounded uniformly for $j \in \mathbb{N}$. Obviously, the mass conservation property is retained by this phase correction. Also, adding an order $\mathrm{O}(\Delta t^3)$ correction at each step does not destroy the overall second order accuracy of the method. With the modulation step (25) we have

$$\frac{|u_j^{(n+1)}|^2}{r_j} = \frac{|u_j^{(n,2)}|^2}{r_j} = -\frac{4\pi}{\gamma} D_r^2 \phi_j^{(n,2)} = -\frac{4\pi}{\gamma} D_r^2 \phi_j^{(n+1)}, \quad j \geq 1, \quad n \geq 0,$$

and using this in (24) we can proceed analogously to the derivation of the energy conservation of the nonlinear scheme and obtain

$$\begin{aligned} D_{t,2}^+ \left[\frac{\hbar^2 \Delta r}{2m} \sum_{j=0}^{J-1} \left| D_r^+ u_j^{(n)} \right|^2 + \frac{\Delta r}{2} \sum_{j=1}^{J-1} \frac{\phi_j^{(n)}}{r_j} \left| u_j^{(n)} \right|^2 \right] \\ = \frac{\Delta r}{2} \sum_{j=1}^{J-1} \frac{\phi_j^{(n,2)} - \phi_j^{(n,1)}}{r_j} D_{t,2}^+ \left| u_j^{(n)} \right|^2 + \frac{\hbar^2}{m} \operatorname{Re}\Big\{ (D_{t,2}^+ \bar{u}_J^{(n)}) D_r^- S_{t,2} u_J^{(n)} \Big\} \\ + \frac{2\pi}{\gamma} \Big((S_{t,2}\phi_J^{(n)}) D_{t,2}^+ D_r^- \phi_J^{(n)} - (D_r^- S_{t,2}\phi_J^{(n)}) D_{t,2}^+ \phi_J^{(n)} \Big). \end{aligned} \tag{26}$$

Next we want to discuss the choice of the *modulation parameter* $\omega \in \mathbb{R}$ and the *modulation function* $g_j = g(r_j) \in \mathbb{R}$ in (25). From (26) we conclude (by

letting $J \to \infty$) the temporal evolution of the *discrete total energy* $E^{(n)}$ as

$$D_{t,2}^{+} \underbrace{\left[\frac{\hbar^2 \Delta r}{2m} \sum_{j \in \mathbb{N}_0} \left| D_r^{+} u_j^{(n)} \right|^2 + \frac{\Delta r}{2} \sum_{j \in \mathbb{N}} \frac{\phi_j^{(n)}}{r_j} \left| u_j^{(n)} \right|^2 \right]}_{=: E^{(n)}} = \frac{\Delta r}{2} \sum_{j \in \mathbb{N}} \frac{\phi_j^{(n,2)} - \phi_j^{(n,1)}}{r_j} D_{t,2}^{+} \left| u_j^{(n)} \right|^2 .$$

With the modulation step (25) we obtain for the *residual* $R^{(n)} := E^{(n+1)} - E^{(n)}$

$$\begin{aligned} R^{(n)} &= E^{(n+1)} - E^{(n,2)} + \Delta t D_{t,2}^{+} E^{(n)} \\ &= \frac{\hbar^2 \Delta r}{2m} \sum_{j \in \mathbb{N}_0} \left(\left| D_r^{+} u_j^{(n+1)} \right|^2 - \left| D_r^{+} u_j^{(n,2)} \right|^2 \right) + \frac{\Delta t}{2} \sum_{j \in \mathbb{N}} \frac{\phi_j^{(n,2)} - \phi_j^{(n,1)}}{j} D_{t,2}^{+} \left| u_j^{(n)} \right|^2 . \end{aligned} \tag{27}$$

The parameter ω is now chosen such that the residual $R^{(n)} = R^{(n)}(\omega)$ in (27) vanishes identically. This involves the solution of a single scalar nonlinear equation for ω. A simple direct calculation now gives:

$$\begin{aligned} \left| D_r^{+} u_j^{(n+1)} \right|^2 - \left| D_r^{+} u_j^{(n,2)} \right|^2 &= \frac{2}{\Delta r^2} \operatorname{Re} \left\{ \bar{u}_j^{(n,2)} u_{j+1}^{(n,2)} - \bar{u}_j^{(n+1)} u_{j+1}^{(n+1)} \right\} \\ &= \frac{2}{\Delta r^2} \operatorname{Re} \left\{ \bar{u}_j^{(n,2)} u_{j+1}^{(n,2)} \left[1 - \exp\left(i \Delta t^3 \omega (g_{j+1} - g_j) \right) \right] \right\} \\ &= -\frac{2 \Delta t^3 \omega}{\Delta r} (D_r^{+} g_j) \operatorname{Re} \left\{ i \bar{u}_j^{(n,2)} u_{j+1}^{(n,2)} \right\} + \mathrm{O}(\Delta t^6) \\ &= -2 \Delta t^3 \omega (D_r^{+} g_j) \operatorname{Re} \left\{ i \bar{u}_j^{(n,2)} D_r^{+} u_j^{(n,2)} \right\} + \mathrm{O}(\Delta t^6), \end{aligned}$$

i.e. in leading order in Δt the parameter ω is given by

$$\omega = \frac{m \sum\limits_{j \in \mathbb{N}} \frac{\phi_j^{(n,2)} - \phi_j^{(n,1)}}{r_j} D_{t,2}^{+} \left| u_j^{(n)} \right|^2}{2 \hbar^2 \Delta t^2 \sum\limits_{j \in \mathbb{N}_0} F_j (D_r^{+} g_j)} + \mathrm{O}(\Delta t), \tag{28}$$

with F_j (the flux) given by

$$F_j = \operatorname{Re} \left\{ i \bar{u}_j^{(n,2)} D_r^{+} u_j^{(n,2)} \right\}, \quad j \in \mathbb{N}_0. \tag{29}$$

Equation (28) can be used as an initial guess for a (scalar) Newton iteration to determine ω by solving (27) with $R^{(n)}(\omega) = 0$.

We note, that the modulation function g should be chosen such that $(D_r^{+} g_j)$ is not orthogonal to F_j everywhere (this does not work for $F_j \equiv 0$ when the reduced wave function $u_j^{(n,2)}$ is purely real or purely imaginary. A simple *first*

idea would be to choose g as some bounded function like a trigonometric function or e.g. $g(r) = 1/(1+r)$.

For a *second approach* [21] we write the wave function in amplitude and phase representation as

$$u_j^{(n,2)} = a_j \exp(ib_j), \quad j \in \mathbb{N}_0, \tag{30}$$

and obtain for the flux

$$F_j = \mathrm{Re}\left\{ia_j\, a_{j+1} \exp(iD_r^+ b_j)\right\} = -a_j\, a_{j+1} \sin(D_r^+ b_j), \quad j \in \mathbb{N}_0, \tag{31}$$

which suggests the choice $g_j = b_j = \arg u_j^{(n,2)}$ for the modulation function.

Finally, as a *third idea* we apply the summation by parts rule to the denominator in (28):

$$\sum_{j\in\mathbb{N}_0} F_j(D_r^+ g_j) = -\sum_{j\in\mathbb{N}} g_j(D_r^- F_j) = -\sum_{j\in\mathbb{N}} g_j\, \mathrm{Re}\left\{iD_r^-(\bar{u}_j^{(n,2)} u_{j+1}^{(n,2)})\right\}, \tag{32}$$

i.e. one obvious possible choice of g_j would be

$$g_j = -\,\mathrm{Re}\left\{iD_r^-(\bar{u}_j^{(n,2)} u_{j+1}^{(n,2)})\right\} = \mathrm{Im}\left\{D_r^+(\bar{u}_{j-1}^{(n,2)} u_j^{(n,2)})\right\}, \tag{33}$$

such that one would sum up square numbers in the denominator. Thus the denominator in (28) can always be made non–zero if u is neither purely real nor purely imaginary.

Remark 2 *In the (rather rare) time steps for which either the real or the imaginary part of u becomes too small and the* modulation strategy *breaks down one has to solve the full nonlinear Crank–Nicolson scheme* (10) *which incidentally is an acceptable computational cost.*

Since the problem (5a) is posed on an unbounded domain we have to introduce an artificial boundary at $j = J$ for the numerical solution. Here we use the approach of a *discrete transparent boundary condition* (DTBC) from [1] which was derived for the linear Schrödinger equation under the assumption that the potential term $V_j^{(n)} = \phi_j^{(n)}/r_j = \text{const}$ for $j \geq J$ (exterior domain). In the following section we will review this approach to clarify the basic ideas and then extend these calculations to the case of a Newton–type potential, i.e. $\phi_j^{(n)}/r_j \sim \text{const}\,/r_j$, $j \to \infty$. It will turn out out that the DTBC for zero potential is the lowest order approximation to the DTBC for the Newton–type potential. Both approaches for the DTBC are used in the example of §5.

3 The Discrete Transparent Boundary Conditions

To derive the DTBC for (5a) we make the *basic assumption* that the initial data $u^I = u(r,0)$ is supported in the computational domain $r < R$. A strategy to overcome this restriction could be found in [9].

3.1 Case of a constant potential term outside the computational domain. We start with assuming that $V(r,t) = \phi(r,t)/r = V_R$ for $r \geq R$.

The transparent boundary condition. The first step is to cut the original problem (5a) into two subproblems, the interior problem on $r < R$, and an exterior problem. They are coupled by the assumption that u, u_r are continuous across the artificial boundary at $r = R$. The *interior problem* reads

$$\begin{aligned} i\partial_t u(r,t) &= -\frac{1}{2m}\partial_r^2 u(r,t) + \frac{\phi(r,t)}{r}u(r,t), \qquad 0 < r < R, \quad t > 0, \\ u(r,0) &= u^I(r), \qquad 0 < r < R, \\ u_r(R,t) &= (T_R u)(R,t). \end{aligned} \tag{34}$$

T_R denote the Dirichlet–to–Neumann map at the boundary, which is obtained by solving the *exterior problem*:

$$\begin{aligned} i\partial_t v &= -\frac{1}{2m}\partial_r^2 v + V_R v, \qquad r > R, \quad t > 0, \\ v(r,0) &= 0, \qquad r > R, \\ v(R,t) &= \Phi(t), \qquad t > 0, \qquad \Phi(0) = 0, \\ \lim_{r\to\infty} v(r,t) &= 0, \\ (T_R\Phi)(t) &= v_r(R,t). \end{aligned} \tag{35}$$

Since the potential $V_R = \phi_\infty/R$ is constant in the exterior problem, we can obtain the boundary operator T_R needed in (34) by solving it explicitly by the Laplace transformation:

$$\hat{v}(r,s) = \int_0^\infty v(r,t)e^{-st}\,dt,$$

where we set $s = \eta + i\xi$, $\xi \in \mathbb{R}$, and $\eta > 0$ is fixed, with the idea to later perform the limit $\eta \to 0$. Now the exterior problem (35) is transformed to

$$\begin{aligned} &\partial_r^2 \hat{v} + 2im\Big(s + iV_R\Big)\hat{v} = 0, \quad r > R, \\ &\hat{v}(R,s) = \hat{\Phi}(s). \end{aligned} \tag{36}$$

Since its solutions have to decrease as $r \to \infty$, we obtain

$$\hat{v}(r,s) = e^{-\sqrt[+]{-2im(s+iV_R)}(r-R)}\hat{\Phi}(s). \tag{37}$$

Hence the Laplace–transformed Dirichlet–to–Neumann operator T_R reads

$$\widehat{T_R\Phi}(s) = \partial_r \hat{v}(R,s) = -\sqrt{2m}\, e^{-i\frac{\pi}{4}} \sqrt[+]{s + iV_R}\hat{\Phi}(s). \tag{38}$$

Here, $\sqrt[+]{\ }$ denotes the branch of the square root with nonnegative real part. Finally, an inverse Laplace transformation yields the TBC at $r = R$:

$$u_r(R,t) = -\sqrt{\frac{2m}{\pi}}\, e^{-i\frac{\pi}{4}} e^{-iV_R t} \frac{d}{dt} \int_0^t \frac{u(R,\tau)\, e^{iV_R\tau}}{\sqrt{t-\tau}}\, d\tau, \tag{39}$$

This boundary condition is non–local in t (of memory–type), thus requiring the storage of all previous time levels at $r = R$ in a numerical discretization.

The discrete TBC. Now we describe how to incorporate the TBC (39) into the Crank–Nicolson finite difference scheme (10a). Instead of using an ad–hoc discretization of the analytic TBC with its mildly singular convolution kernel (*discretized TBC*) which is on the discrete level not perfectly transparent any more and may also yield an unstable numerical scheme we will construct a *discrete TBC* of the fully discretized problem. Our strategy solves both problems of the *discretized TBC* at no additional computational costs. With our DTBC the numerical solution on the computational domain $0 \le j \le J$ equals the discrete solution on $j \in \mathbb{N}$ restricted to the domain $0 \le j \le J$. Therefore, our overall scheme avoids any numerical reflections at the boundary and inherits the unconditional stability of the Crank–Nicolson scheme.

We rewrite the scheme (10a) in the form:

$$-i\rho(u_j^{(n+1)} - u_j^{(n)}) = \Delta^2(u_j^{(n+1)} + u_j^{(n)}) + w\frac{\phi_j^{(n+\frac{1}{2})}}{r_j}(u_j^{(n+1)} + u_j^{(n)}), \tag{40}$$

with the second order difference operator $\Delta^2 u_j^{(n)} = \Delta r^2 D_r^2 u_j^{(n)}$ and the ratios

$$\rho = \frac{4m}{\hbar}\frac{\Delta r^2}{\Delta t}, \qquad w = -\frac{2m}{\hbar^2}\Delta r^2.$$

To derive the discrete TBC we will now mimic the derivation of the analytic TBC on a discrete level. In analogy to the continuous problem we assume: $\phi_j^{(n+\frac{1}{2})}/r_j = V_R = \text{const}$, $u_j^0 = 0$, $j \ge J-1$, and solve the discrete exterior problem by using the Z–transformation:

$$\mathcal{Z}\{u_j^{(n)}\} = \hat{u}_j(z) := \sum_{n=0}^{\infty} u_j^{(n)}\, z^{-n}, \quad z \in \mathbb{C}, \quad |z| > 1.$$

Hence, the Z–transformed finite difference scheme (40) for $j \ge J$ reads

$$(z+1)\Delta^2 \hat{u}_j(z) = -i\rho\Big[z - 1 + i\kappa(z+1)\Big]\hat{u}_j(z), \quad \kappa = \frac{\Delta t}{2}\frac{V_R}{\hbar}. \tag{41}$$

The two linearly independent solutions of this second order difference equation (41) take the form $\hat{u}_j(z) = \nu_{1,2}^j(z)$, $j \geq J$, where $\nu_{1,2}(z)$ solve

$$\nu^2 - 2\left[1 - \frac{i\rho}{2}\Big(\frac{z-1}{z+1} + i\kappa\Big)\right]\nu + 1 = 0. \tag{42}$$

For the decreasing mode (as $j \to \infty$) we have to require $|\nu_1(z)| < 1$ and obtain the Z–transformed DTBC as

$$\hat{u}_{J-1}(z) = \nu_1^{-1}(z)\,\hat{u}_J(z). \tag{43}$$

It only remains to inverse transform (43) and in a tedious calculation this can be achieved explicitly [1]. However, since the magnitude of $\ell^{(n)} := \mathcal{Z}^{-1}\{\nu_1^{-1}(z)\}$ does not decay as $n \to \infty$ ($\operatorname{Im}\ell^{(n)}$ behaves like const $\cdot(-1)^n$ for large n), it is more convenient to use a modified formulation of the DTBC (cf. [9]). Therefore we introduce the *summed coefficients*

$$s^{(n)} = \mathcal{Z}^{-1}\{\hat{s}(z)\}, \text{ with } \hat{s}(z) := \frac{z+1}{z}\hat{\ell}(z), \tag{44}$$

which satisfy

$$s^{(0)} = \ell^{(0)}, \quad s^{(n)} = \ell^{(n)} + \ell^{(n-1)}, \quad n \geq 1.$$

The discrete TBC (at $j = J$) for the discretization (40) now reads (cf. [1]):

$$u_{J-1}^{(n)} - s^{(0)}u_J^{(n)} = \sum_{k=1}^{n-1} s^{(n-k)}u_J^{(k)} - u_{J-1}^{n-1}, \quad n \geq 1, \tag{45}$$

with

$$s^{(n)} = \Big[1 - i\frac{\rho}{2} + \frac{\sigma}{2}\Big]\delta_n^0 + \Big[1 + i\frac{\rho}{2} + \frac{\sigma}{2}\Big]\delta_n^1 + \alpha\, e^{-in\varphi}\,\frac{P_n(\mu) - P_{n-2}(\mu)}{2n-1}\,,$$

$$\varphi = \arctan\frac{2\rho(\sigma+2)}{\rho^2 - 4\sigma - \sigma^2}, \quad \mu = \frac{\rho^2 + 4\sigma + \sigma^2}{\sqrt{(\rho^2+\sigma^2)(\rho^2 + [\sigma+4]^2)}}, \tag{46}$$

$$\sigma = -wV_R, \quad \alpha = \frac{i}{2}\sqrt[4]{(\rho^2+\sigma^2)(\rho^2+[\sigma+4]^2)}\,e^{i\varphi/2}.$$

P_n denotes the Legendre polynomials ($P_{-1} \equiv P_{-2} \equiv 0$) and δ_n^j the Kronecker symbol. The P_n only have to be evaluated at one value $\mu \in \mathbb{R}$, and hence the numerically stable recursion formula for the Legendre polynomials can be used. Using asymptotic properties of the Legendre polynomials one finds $s^{(n)} = \mathrm{O}(n^{-3/2})$, which agrees with the decay of the convolution kernel in the differential TBC (39) (after an integration by parts).

3.2 Case of a Coulomb–like potential term outside the computational domain. We now assume that $V(r,t) = \phi_\infty/r$ for $r \geq R$ with $\phi_\infty = \frac{\gamma}{4\pi}$.

The transparent boundary condition. We briefly repeat the analogous steps for this case. The transformed exterior problem now reads

$$\begin{aligned} &\partial_r^2 \hat{v} + 2im\Big(s + i\frac{\phi_\infty}{r}\Big)\hat{v} = 0, \quad r > R, \\ &\hat{v}(R,s) = \hat{\Phi}(s). \end{aligned} \tag{47}$$

The solution of this second order ODE that decreases as $r \to \infty$ is given by *Whittaker's second function* [15]:

$$\hat{v}(r,s) = \frac{W_{\mu,\frac{1}{2}}(\alpha(s)r)}{W_{\mu,\frac{1}{2}}(\alpha(s)R)}\,\hat{\Phi}(s), \tag{48}$$

with

$$\alpha(s) = 2\sqrt{2m}\,e^{-i\frac{\pi}{4}}\,\sqrt[+]{s}, \quad \mu(s) = \frac{\phi_\infty}{4is}\alpha(s) = -\frac{\sqrt{m}\,e^{i\frac{\pi}{4}}\,\phi_\infty}{\sqrt{2}\,\sqrt[+]{s}}.$$

Hence the Laplace–transformed Dirichlet–to–Neumann operator T_R reads

$$\widehat{T_R\Phi}(s) = \partial_r \hat{v}(R,s) = \alpha(s)\frac{W'_{\mu,\frac{1}{2}}(\alpha(s)R)}{W_{\mu,\frac{1}{2}}(\alpha(s)R)}\hat{\Phi}(s). \tag{49}$$

For applying the inverse Laplace transformation we have to use an asymptotic expansion for μ fixed, $r \to \infty$ [15]:

$$W_{\mu,\frac{1}{2}}(z) \approx e^{-\frac{z}{2}} z^{\mu}\ {}_2\mathrm{F}_0(1-\mu,-u;;-\frac{1}{z}), \quad -\frac{3\pi}{2} < \arg z < \frac{3\pi}{2}. \tag{50}$$

The hypergeometric function ${}_2\mathrm{F}_0$ in (50) is given by:

$${}_2\mathrm{F}_0(1-\mu,-u;;-\frac{1}{z}) = \sum_{k=0}^{\infty} \frac{(1-\mu)_k(-\mu)_k}{k!}(-1)^k z^{-k}, \quad |z| > 1, \tag{51}$$

with the Pochhammer notation

$$(\mu)_0 = 1, \quad (\mu)_k = \mu(\mu+1)\cdot\cdots\cdot(\mu+k-1) = \frac{\Gamma(\mu+k)}{\Gamma(\mu)}.$$

If we use e.g. the lowest order approximation $W_{\mu,\frac{1}{2}}(z) \approx e^{-\frac{z}{2}} z^{\mu}$ we obtain

$$\widehat{T_R\Phi}(s) = \partial_r \hat{v}(R,s) = \Big(-\frac{\alpha(s)}{2} + \frac{\mu(s)}{R}\Big)\hat{\Phi}(s). \tag{52}$$

Finally, an inverse Laplace transformation yields the TBC at $r = R$:

$$u_r(R,t) = -\sqrt{\frac{2m}{\pi}}\,e^{-i\frac{\pi}{4}} \int_0^t \frac{u_t(R,\tau) + \frac{i}{2}\frac{\phi_\infty}{R}\,u(R,\tau)}{\sqrt{t-\tau}}\,d\tau. \tag{53}$$

Again, like (39), the condition (53) is non–local in time with a mildly singular kernel and we prefer to derive a discrete TBC directly on the discrete level.

The discrete TBC. We now proceed deriving a discrete version of the TBC (53). In analogy to the continuous problem we assume: $\phi_j^{(n)} = \phi_j^{(n,1)} = \phi_j^{(n,2)} = \phi_\infty$, $u_j^0 = 0$, $j \geq J-1$, and write the discrete Z–transformed exterior problem (40) as

$$\hat{u}_{j+1}(z) + \hat{u}_{j-1}(z) = 2\Big[1 - i\rho\frac{z-1}{z+1} + \frac{m\Delta r}{\hbar^2}\frac{\phi_\infty}{j}\Big]\hat{u}_j(z), \quad j \geq J. \tag{54}$$

Motivated by (43), we want to obtain the *transformed DTBC* in the form:

$$\hat{u}_{J-1}(z) = \hat{\ell}(z)\,\hat{u}_J(z). \tag{55}$$

Unfortunately, the exact solution to (54) is not known explicitly In the sequel we will construct some expressions for $\hat{\ell}(z)$ by determining asymptotic solutions to (54) through different approaches.

First of all, following the *approach of Mickens* [17], the asymptotic solution of

$$\hat{u}_{j+1}(z) + \hat{u}_{j-1}(z) = 2\Big[A_0 + \frac{A_1}{j}\Big]\hat{u}_j(z), \quad j \geq J, \tag{56}$$

takes the form

$$\hat{u}_j(z) \sim j^\theta e^{B_0 j}\Big[1 + \sum_{k=1}^{\infty}\frac{B_k}{j^k}\Big], \tag{57}$$

where the parameters θ and B_k are expressible in terms of $A_0 = A_0(z)$, A_1. The parameters θ, B_0, B_1 can be obtained by

$$\cosh(B_0) = A_0, \text{ i.e. } B_0 = \ln\Big(A_0 \pm \sqrt{A_0^2 - 1}\Big), \tag{58a}$$

$$\theta = \frac{A_1}{\sinh(B_0)}, \tag{58b}$$

$$B_1 = \frac{\theta(\theta-1)}{2}\coth(B_0). \tag{58c}$$

In our case we obtain

$$e^{B_0} = \nu_1(z), \tag{59a}$$

$$\theta = \frac{2m\Delta r}{\hbar^2}\frac{\phi_\infty}{\nu_1(z) - \nu_1^{-1}(z)}, \tag{59b}$$

$$B_1 = \frac{\theta(\theta-1)}{2}\frac{\nu_1(z) + \nu_1^{-1}(z)}{\nu_1(z) - \nu_1^{-1}(z)}, \tag{59c}$$

where $\nu_1(z)$ is the solution to (42) for the Schrödinger equation with zero potential (i.e. $\kappa = 0$) with $|\nu_1(z)| < 1$.

Secondly, one can use the *approach of Wong and Li* [25] to obtain a formula for the asymptotic behaviour of the solutions to this second order difference equation. This is possible since equation (54) is of *Poincaré type*, i.e. the

coefficients in (54) have finite limits for $j \to \infty$. To do so, we rewrite (54) in the form

$$\hat{u}_{j+2} + a(j)\,\hat{u}_{j+1} + \hat{u}_j = 0, \quad j \geq J, \tag{60}$$

with $a(j) = -2[A_0 + A_1/(j+1)]$. Now $a(j)$ has a power expansion of the form

$$a(j) = \sum_{k=0}^{\infty} \frac{a_k}{j^k},$$

with coefficients:

$$a_0 = -2A_0, \quad a_k = 2A_1(-1)^k, \quad k \geq 1.$$

Then the decaying asymptotic solution (cf. [25]) is of the form

$$\hat{u}_j \sim \nu_1(z)^j j^\alpha \sum_{k=0}^{\infty} \frac{c_k}{j^k}, \qquad j \to \infty, \tag{61}$$

where α can be calculated as

$$\alpha = \frac{a_1\nu_1(z)}{a_0\nu_1(z)+2} = \frac{A_1\nu_1(z)}{A_0\nu_1(z)-1} = \frac{2A_1}{\nu_1(z)-\nu_1^{-1}(z)}. \tag{62}$$

Without loss of generality, we assume that $c_0 = 1$ and determine the values of the coefficients c_1, $c_2, \ldots$ by formula (2.3) in [25] or more illustrative by substituting the solution (61) in (60):

$$\nu_1^2\Big(1+\frac{2}{j}\Big)^\alpha \sum_{k=0}^{\infty} \frac{c_k}{(j+2)^k} + a(j)\nu_1\Big(1+\frac{1}{j}\Big)^\alpha \sum_{k=0}^{\infty} \frac{c_k}{(j+1)^k} + \sum_{k=0}^{\infty} \frac{c_k}{j^k} = 0.$$

We now obtain after a Taylor expansion in $1/j$ and setting all the linearly independent terms equal to zero, by a lengthy but elementary calculation

$$c_1 = \frac{\alpha^2 + A_0A_1\alpha - \alpha - A_1\nu + A_1^2}{2(A_0\nu - 1)}, \tag{63a}$$

$$c_2 = \frac{c_1^2}{2} + \frac{A_0\nu - \alpha}{2(A_0\nu-1)}\,c_1 + \frac{1 - A_1\nu - A_0A_1 - A_0^2}{3(A_0\nu-1)}\,c_1 + \frac{(A_0^3c_1 + \nu - A_0)A_1}{6(A_0\nu-1)} + \frac{(A_0^2 - A_1\nu + A_1A_0 - 3)A_1^2}{12(A_0\nu-1)}, \tag{63b}$$

etc..

This result can be checked easily with a symbolic package like MAPLE. We note that after some basic manipulations one observes that these two approaches lead to the same asymptotic solution of the difference equation (54).

Finally, for a third approach to construct an approximation to the DTBC, we use a formulation as a *continued fraction*. One can deduce such expression for the quotient $\hat{\ell}(z) = \hat{u}_{J-1}(z)/\hat{u}_J(z)$ as a continued fraction directly from the

difference scheme (54). This approach is often better than evaluating the quotient of two asymptotic solutions (obtained by any of the previous approaches) at two neighboured grid points. If we rewrite (54) as

$$\frac{\hat{u}_{J-1}(z)}{\hat{u}_J(z)} = 2\Big[A_0 + \frac{A_1}{j}\Big] - \frac{1}{\frac{\hat{u}_J(z)}{\hat{u}_{J+1}(z)}},$$

it is obvious that

$$\frac{\hat{u}_{J-1}(z)}{\hat{u}_J(z)} = 2\Big[A_0 + \frac{A_1}{J}\Big] - \frac{1}{2[A_0 + \frac{A_1}{J+1}]} - \cdots - \frac{1}{2[A_0 + \frac{A_1}{J+M}]} - \frac{\hat{u}_{J+M+1}(z)}{\hat{u}_{J+M}(z)}.$$

For decreasing solutions the last quotient may be neglected when $M \to \infty$, i.e. we obtain the expansion

$$\hat{\ell}(z) = 2\Big[A_0 + \frac{A_1}{J}\Big] - \frac{1}{2[A_0 + \frac{A_1}{J+1}]} - \frac{1}{2[A_0 + \frac{A_1}{J+2}]} - \cdots. \tag{64}$$

This continued fractions formula (64) offers another way to evaluate the quotient $\hat{\ell}(z)$ needed in the transformed discrete TBC (43). For the numerical implementation we use the *modified Lentz's method* [13] which is an efficient general method for evaluating continued fractions. We remark that this approach is suitable for general second order difference equations.

Remark 3 *Our practical calculations in §5 showed that the evaluation of the continued fraction* (64) *is stable for all considered values of* A_0 *and* A_1 *although we cannot prove this yet.*

We finish this section with a short note about the implementation of the discrete TBC using the above approaches. As in the case for the constant potential in the exterior domain (cf. (44)) it is favourable to use

$$\hat{s}(z) := \frac{z+1}{z}\,\hat{\ell}(z). \tag{65}$$

An inverse Z–transformation yields finally the *discrete TBC*

$$u_{J-1}^{(n)} - s^{(0)} u_J^{(n)} = \sum_{k=1}^{n-1} s^{(n-k)} u_J^{(k)} - u_{J-1}^{(n-1)}, \quad n \geq 1. \tag{66}$$

with

$$s^{(n)} = \mathcal{Z}^{-1}\{\hat{s}(z)\} = \frac{\tau^n}{2\pi} \int_0^{2\pi} \hat{s}(\tau e^{i\varphi}) e^{in\varphi}\, d\varphi, \quad n \in \mathbb{Z}_0, \quad \tau > 0. \tag{67}$$

Since this inverse Z–transformation cannot be done explicitly, we use a numerical inversion technique based on FFT (cf. [9]); for details of this routine we refer the reader to [8].

Remark 4 *As noted before, this DTBC* (66) *can also used for both the predictor* (20a) *and the corrector step* (21a) *for the Schrödinger equation. In the exterior domain they are*

$$i\hbar D^+_{t,k} u_j^{(n)} = -\frac{\hbar^2}{2m} D_r^2 S_{t,k} u_j^{(n)} + \frac{\phi_\infty}{r_j} S_{t,k} u_j^{(n)}, \quad j \geq J, \tag{68}$$

$k = 1, 2$, *i.e. after a (slightly modified) Z–transformation they are of the form* (54) *and a DTBC analogue to* (66) *can be applied.*

4 Approximation by Sums of Exponentials

An ad–hoc implementation of the discrete convolution (66) with convolution coefficients $s^{(n)}$ (obtained by any of the above approaches) has still one disadvantage. The boundary condition is non–local and therefore computationally expensive especially for long–time calculations. In fact, evaluating the convolution appearing in the exact discrete TBC (66) (or (45)), becomes with increasing time more expensive than solving the whole interior scheme. As a remedy, we proposed in [2] the sum–of–exponentials ansatz. While the computational effort for the discrete TBC is quadratic in time, the effort for the approximated discrete TBC only increases linearly. In the sequel we will briefly review this approach.

4.1 The Sum–of–Exponentials Ansatz. In order to derive a fast numerical method to calculate the discrete convolution in (66), we approximate the coefficients $s^{(n)}$ by the following (*sum of exponentials*):

$$s^{(n)} \approx \tilde{s}^{(n)} := \begin{cases} s^{(n)}, & n = 0, 1 \\ \displaystyle\sum_{l=1}^{L} b_l \, q_l^{-n}, & n = 2, 3, \dots, \end{cases} \tag{69}$$

where $L \in \mathbb{N}$ is a fixed number (e.g. $L = 20$). Evidently, the approximation properties of $\tilde{s}^{(n)}$ depend on L, and the corresponding set $\{b_l, q_l\}$. We remark that the computational effort does not change considerably for different values of L since the evaluation of the sum-of-exponential convolutions has a negligible effort compared to solving the PDE in the interior domain. Below we propose a deterministic method of finding $\{b_l, q_l\}$ for fixed L.

Let us fix L and consider the formal power series:

$$g(x) := s^{(2)} + s^{(3)} x + s^{(4)} x^2 + \dots, \quad |x| \leq 1. \tag{70}$$

If there exists the $[L-1|L]$ *Padé approximation* $\tilde{g}(x) := P_{L-1}(x)/Q_L(x)$ of

(70), then its Taylor series

$$\tilde{g}(x) = \tilde{s}^{(2)} + \tilde{s}^{(3)}x + \tilde{s}^{(4)}x^2 + \dots$$

satisfies the conditions

$$\tilde{s}^{(n)} = s^{(n)}, \qquad n = 2, 3, \dots, 2L+1, \tag{71}$$

due to the definition of the Padé approximation rule.

Theorem 5 ([2]) *Let $Q_L(x)$ have L simple roots q_l with $|q_l| > 1$, $l = 1, \dots, L$. Then*

$$\tilde{s}^{(n)} = \sum_{l=1}^{L} b_l \, q_l^{-n}, \qquad n = 2, 3, \dots , \tag{72}$$

where

$$b_l := -\frac{P_{L-1}(q_l)}{Q'_L(q_l)} \, q_l \neq 0, \qquad l = 1, \dots, L.$$

It follows from (71) and (72) that the set $\{b_l, q_l\}$ defined in Theorem 5 can be used in (69) at least for $n = 2, 3, .., 2L+1$. The main question now is: Is it possible to use these $\{b_l, q_l\}$ also for $n > 2L+1$? In other words, what quality of approximation

$$\tilde{s}^{(n)} \approx s^{(n)}, \qquad n > 2L+1$$

can we expect?

The above analysis permits us to give the following description of the approximation to the convolution coefficients $s^{(n)}$ by the representation (69) if we use a $[L-1|L]$ Padé approximant to (70): the first $2L$ coefficients are reproduced exactly, see (71); however, the asymptotic behaviour of $s^{(n)}$ and $\tilde{s}^{(n)}$ (as $n \to \infty$) differs strongly (algebraic versus exponential decay). A typical graph of $|s^{(n)} - \tilde{s}^{(n)}|$ versus n for the DTBC of §3.2 and $L = 30$ is shown in Fig. 3 in Section 5.

4.2 Fast Evaluation of the Discrete Convolution. Let us consider the approximation (69) of the discrete convolution kernel appearing in the DTBC (66). With these "exponential" coefficients the convolution

$$C^{(n)} := \sum_{k=1}^{n-1} \tilde{s}^{(n-k)} u_J^{(k)}, \quad \tilde{s}^{(n)} = \sum_{l=1}^{L} b_l \, q_l^{-n}, \tag{73}$$

$|q_l| > 1$, of a discrete function $u_J^{(k)}$, $k = 1, 2, \dots$, with the kernel coefficients $\tilde{s}^{(n)}$, can be calculated by recurrence formulas, and this will reduce the numerical effort significantly.

A straightforward calculation (cf. [2]) yields: The value $C^{(n)}$ from (73) for

$n \geq 2$ is represented by

$$C^{(n)} = \sum_{l=1}^{L} C_l^{(n)},$$

where $C_l^{(1)} \equiv 0$ and

$$C_l^{(n)} = q_l^{-1} C_l^{(n-1)} + b_l \, q_l^{-2} u_J^{(n-2)}, \quad n = 2, 3, \ldots.$$

Finally, we summarize the approach by the following algorithm:

1. calculate $s^{(n)}, n = 0, \ldots, N-1$, via numerical inverse Z–transformation;
2. calculate $\tilde{s}^{(n)}$ via Padé–algorithm;
3. the corresponding coefficients b_l, q_l are used for the efficient calculation of the discrete convolution.

Remark 6 *We note that the Padé approximation must be performed with high precision ($2L-1$ digits mantissa length) to avoid a 'nearly breakdown' by ill conditioned steps in the Lanczos algorithm (cf. [6]). If such problems still occur or if one root of the denominator is smaller than 1 in absolute value, the orders of the numerator and denominator polynomials are successively reduced.*

5 Numerical Examples

In this section we want to present the results for the numerical integration of the time–dependent Schrödinger–Poisson system (5) in the *attractive case* (i.e. the coupling constant γ is negative) with negative energy. The existence of an analytical breathing mode solution for this case was proven in [23, Section 8] and our long–term objective using the derived DTBCs will be to find discrete breathers. We will compare the results using two different schemes and consider the different proposed strategies for implementing a discrete TBC for the SPS. First we use a *linear Crank–Nicolson scheme*, which is obtained from the nonlinear Crank–Nicolson scheme (10) by using an extrapolation in time for the potential term (which retains the second order accuracy of the scheme):

$$i\hbar D_t^+ u_j^{(n)} = -\frac{\hbar^2}{2m} D_r^2 u_j^{(n+\frac{1}{2})} + \frac{\tilde{\phi}_j^{(n+\frac{1}{2})}}{r_j} u_j^{(n+\frac{1}{2})}, \quad j \geq 1, \tag{74a}$$

$$D_r^2 \phi_j^{(n+1)} = -\frac{\gamma}{4\pi} \frac{\left| u_j^{(n+1)} \right|^2}{r_j}, \quad j \geq 1, \tag{74b}$$

$$\text{with } \tilde{\phi}_j^{(n+\frac{1}{2})} = \frac{3}{2}\phi_j^{(n)} - \frac{1}{2}\phi_j^{(n-1)}. \tag{74c}$$

For this scheme we use the discrete TBC of Section 3.1 and compare it with the results obtained by the predictor–corrector method (20)–(21) together with

the new discrete TBC of Section 3.2 combined with the sum–of–exponentials ansatz (69).

5.1 The discrete Conservation of the Mass and the Energy. The conservation of the mass (11) and the total energy (17) (on $j \geq 0$) provides a useful check of our numerical procedure. We need to clarify how to calculate numerically these conserved quantities which are defined originally on an unbounded domain. We start with the nonlinear Crank–Nicolson scheme (10). For the discrete mass we obtain on the exterior domain $j \geq J$ similar to (15):

$$D_t^+ \Delta r \sum_{j=J}^{\infty} \left| u_j^{(n)} \right|^2 = \frac{\hbar}{m} \operatorname{Im}\Big\{ \bar{u}_J^{(n+\frac{1}{2})} D_r^- u_J^{(n+\frac{1}{2})} \Big\}, \tag{75}$$

and summing up in time for $k = 0, 1 \ldots, n-1$ yields

$$\|u^{(n)}\|_2^2 = \Delta r \sum_{j=1}^{J-1} \left| u_j^{(n)} \right|^2 + \frac{\hbar \Delta t}{m} \operatorname{Im} \sum_{k=0}^{n-1} \bar{u}_J^{(k+\frac{1}{2})} D_r^- u_J^{(k+\frac{1}{2})}. \tag{76}$$

For calculating the energy we obtain an equation similar to (19):

$$\begin{aligned} & D_t^+ \left[\frac{\hbar^2 \Delta r}{2m} \sum_{j=J}^{\infty} \left| D_r^+ u_j^{(n)} \right|^2 + \frac{\Delta r}{2} \sum_{j=J}^{\infty} \frac{\phi_j^{(n)}}{r_j} \left| u_j^{(n)} \right|^2 \right] \\ & = \frac{2\pi}{\gamma} \Big((D_r^- \phi_J^{(n+\frac{1}{2})}) D_t^+ \phi_J^{(n)} - \phi_J^{(n+\frac{1}{2})} D_t^+ D_r^- \phi_J^{(n)} \Big) - \frac{\hbar^2}{m} \operatorname{Re}\Big\{ (D_t^+ \bar{u}_J^{(n)}) D_r^- u_J^{(n+\frac{1}{2})} \Big\}. \end{aligned}$$

Again, summing up with respect to time gives for the discrete total energy

$$\begin{aligned} E^{(n)} = {} & \frac{\hbar^2 \Delta r}{2m} \sum_{j=0}^{J-1} \left| D_r^+ u_j^{(n)} \right|^2 + \sum_{j=1}^{J-1} \frac{\phi_j^{(n)}}{2j} \left| u_j^{(n)} \right|^2 - \frac{\hbar^2 \Delta t}{m} \operatorname{Re} \sum_{k=0}^{n-1} (D_t^+ \bar{u}_J^{(k)}) D_r^- u_J^{(k+\frac{1}{2})} \\ & + \frac{2\pi \Delta t}{\gamma} \sum_{k=0}^{n-1} \Big((D_r^- \phi_J^{(k+\frac{1}{2})}) D_t^+ \phi_J^{(k)} - \phi_J^{(k+\frac{1}{2})} D_t^+ D_r^- \phi_J^{(k)} \Big). \end{aligned} \tag{77}$$

Note that the last boundary term can be simplified:

$$(D_r^- \phi_J^{(k+\frac{1}{2})}) D_t^+ \phi_J^{(k)} - \phi_J^{(k+\frac{1}{2})} D_t^+ D_r^- \phi_J^{(k)} = \frac{\phi_{J-1}^{(k+1)} \phi_J^{(k)} - \phi_{J-1}^{(k)} \phi_J^{(k+1)}}{\Delta t \, \Delta r}.$$

Formulas (76), (77) are used without changes for the linear scheme (74).

For the predictor–corrector scheme (20)–(21) (i.e. without the modulation step (25)) we obtain analogously for the calculation of the mass

$$\|u^{(n)}\|_2^2 = \Delta r \sum_{j=1}^{J-1} \left| u_j^{(n)} \right|^2 + \frac{\hbar \Delta t}{m} \operatorname{Im} \sum_{k=0}^{n-1} (S_{t,2} \bar{u}_J^{(k)}) D_r^- S_{t,2} u_J^{(k)}. \tag{78}$$

Analogously to (77) the discrete total energy is calculated by

$$E^{(n)} = \frac{\hbar^2 \Delta r}{2m} \sum_{j=0}^{J-1} \left| D_r^+ u_j^{(n)} \right|^2 + \sum_{j=1}^{J-1} \frac{\phi_j^{(n)}}{2j} \left| u_j^{(n)} \right|^2 - \frac{\hbar^2 \Delta t}{m} \operatorname{Re} \sum_{k=0}^{n-1} (D_{t,2}^+ \bar{u}_J^{(k)}) D_r^- S_{t,2} u_J^{(k)} + \frac{2\pi}{\gamma \Delta r} \sum_{k=0}^{n-1} \left(\phi_{J-1}^{(k,2)} \phi_J^{(k)} - \phi_{J-1}^{(k)} \phi_J^{(k,2)} \right).$$

5.2 Examples. Here we want to present some numerical results to illustrate the findings of the preceeding sections. The main program is written in MATLAB and the convolution coefficients $s^{(n)}$ are computed by a MAPLE routine (due to the possibility of a simple adaption of the mantissa length, cf. Remark 6 in §4). For simplicity we set $\hbar = 1$ and $m = 1$.

Example 1. First we want to study the convolution coefficients appearing in the different discrete TBCs. We use for the discretization 2000 grid points in radial direction in the computational domain $r < 50$ (i.e. $\Delta r = 1/40$) and a time step $\Delta t = 1/4000$. The coupling constant is set to $\gamma = -64\pi/5$ (cf. [23]).

For these discretization parameters (especially $J = 2000$) it turns out that using the asymptotic solutions (57), (61) is not advisable since for large J we have $\hat{\ell}(z) \sim 2(A_0(z) + A_1/J)$ which is only the first term in the continued fraction expansion (64). Therefore, we decided to calculate the transformed boundary kernel $\hat{\ell}(z)$ in (55) by the continued fraction formula (64) together with the sum–of–exponentials ansatz (69).

We computed the first 1000 terms in the expansion (64) and used a radius $\tau = 1.01$ with 2^{10} sampling points for the numerical inverse Z–transformation (67). Note that the choice of an appropriate radius τ is a delicate problem: it must not be too close to the convergence radius of (64) due to the approximation error but a too large τ raises big rounding errors during the rescaling process. These problems do not exist when using the sum–of–exponentials approximation (since only the first $2L + 1$ exact convolution coefficients are needed). For a detailed discussion of the choice of a suitable radius τ we refer the reader to [2, Section 2] and [26].

First we examine the exact convolution coefficients of the two different DTBCs presented in §3.1 and §3.2. Fig. 1 shows a comparison of the coefficients $s^{(n)}$ from the discrete TBC (45) (constant potential) with the coefficients $s^{(n)}$ from the discrete TBC (66) (Newton–type potential). This illustrates the effect of the potential, when we regard its $1/r$–decay in the exterior domain. The difference of these two sequences of convolution coefficients is shown in Fig. 2. In Fig. 3 we plot both the exact convolution coefficients $s^{(n)}$ and the error $|s^{(n)} - \tilde{s}^{(n)}|$ versus n for $L = 30$ (observe the different scales!).

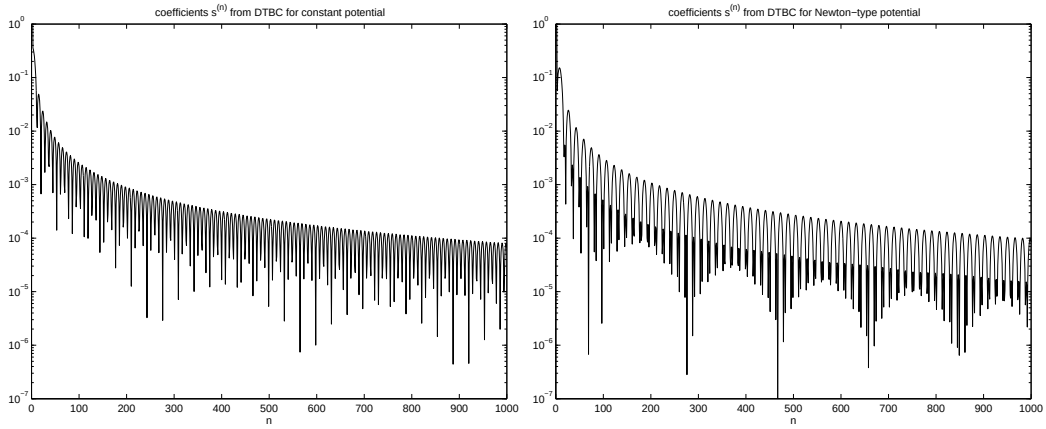

Fig. 1. Comparison of the convolution coefficients $s^{(n)}$ of the discrete TBC (45) (left) and (66) (right).

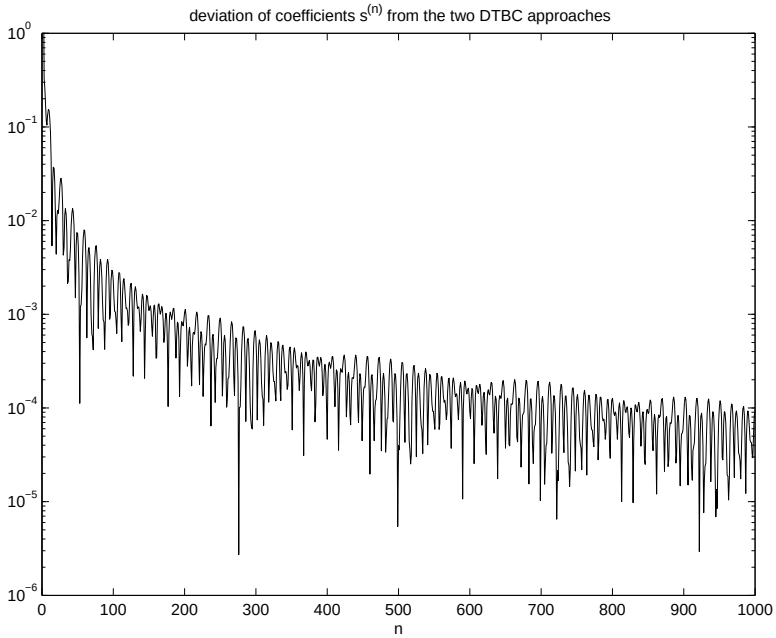

Fig. 2. Deviation of the convolution coefficients $s^{(n)}$ obtained from the two approaches of §3.1 and §3.2.

Example 2. In the second example we want to investigate numerically the conservation properties. We consider the Crank–Nicolson scheme (74) with the discrete TBC (45) and the predictor–corrector method (20)–(21) (i.e. without the modulation step (25)) with the new discrete TBC (66). We choose $\Delta r = 1/20$, $\Delta t = 1/100$ and a computational domain $r < 6$. For a fair comparison we use a time step $\Delta t/2$ for the Crank–Nicolson scheme (74).

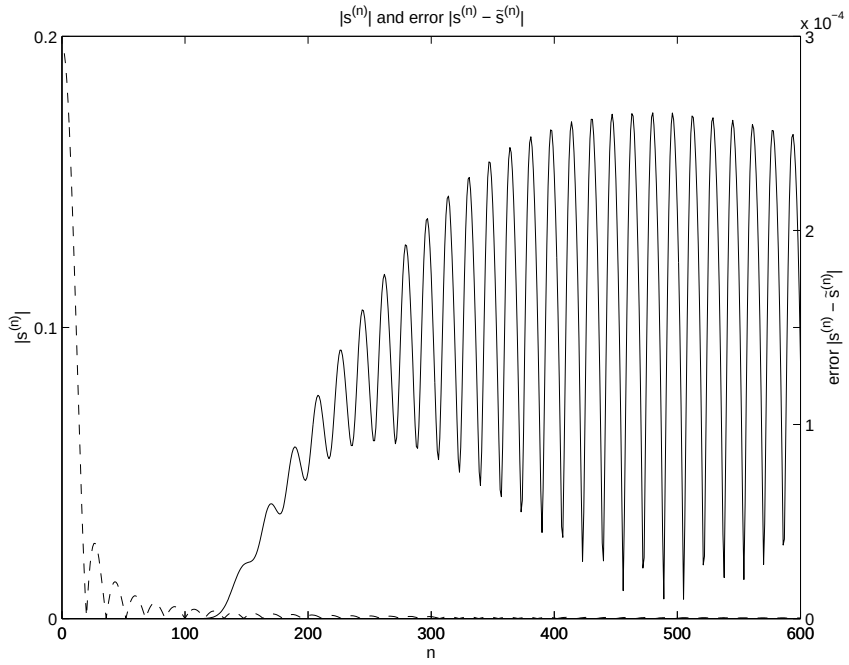

Fig. 3. Convolution coefficients $s^{(n)}$ (left axis, dashed line) and error $|s^{(n)} - \tilde{s}^{(n)}|$ of the convolution coefficients (right axis); ($L = 30$).

Without loss of generality we choose the initial data to be real:

$$u^I(r) = \begin{cases} r\,\exp\Big(-\beta^2/(\beta^2 - r^2)\Big), & r < \beta \\ 0, & \text{else} \end{cases}, \tag{79}$$

with the parameter $\beta = 5.5$ and then normalize u^I such that $\|u^I\|_2 = 1$. We remark that after one predictor–corrector step u is not purely real any more and the initial value of the modulation parameter ω (28) is well–defined. Fig. 4 shows the time evolution of the solution u up to $T = 40$ (i.e. 4000 time steps). One observes the typical oscillating (*'breathing'*) behaviour of the solution u.

The discrete L^2–norm computed by (76), (78) was conserved up to the computational accuracy by both schemes. However, as explained before, there is a spurious gain/loss of the discrete total energy. In Fig. 5 we plotted the total energy for the Crank–Nicolson scheme and the predictor–corrector method. In contrast, the predictor–corrector scheme with the modulation strategy (here we used the third idea (33)) conserves the total energy (up to round–off errors). Note that we have to compute the total energy of the predictor–corrector method with modulation strategy on a sufficiently large domain since the formulas of §5.1 with the boundary terms do not hold.

We use the different proposed modulation functions g_j for the phase correction step (25). The initial value ω_0 for the Newton iteration to determine the

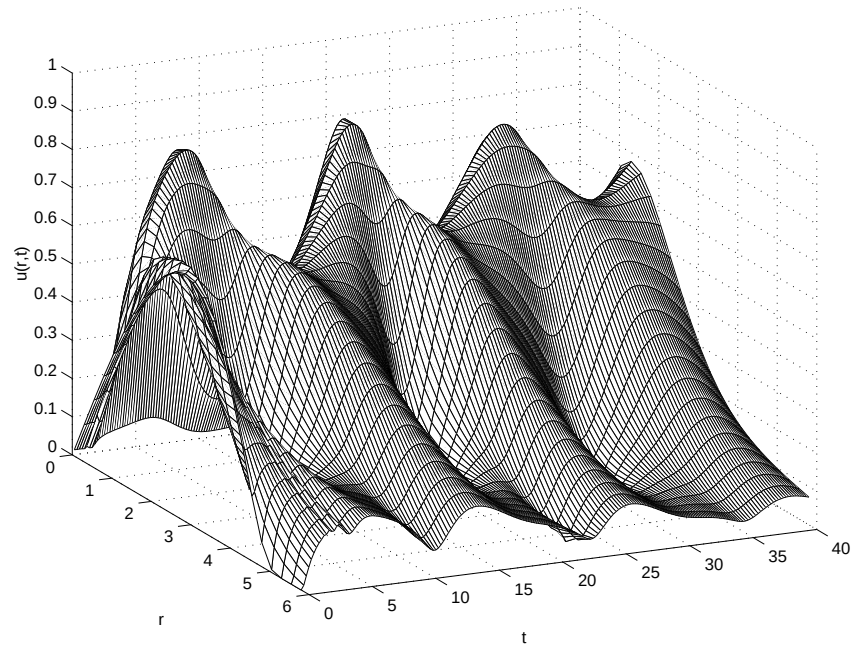

Fig. 4. Time evolution of the solution u up to $T = 40$.

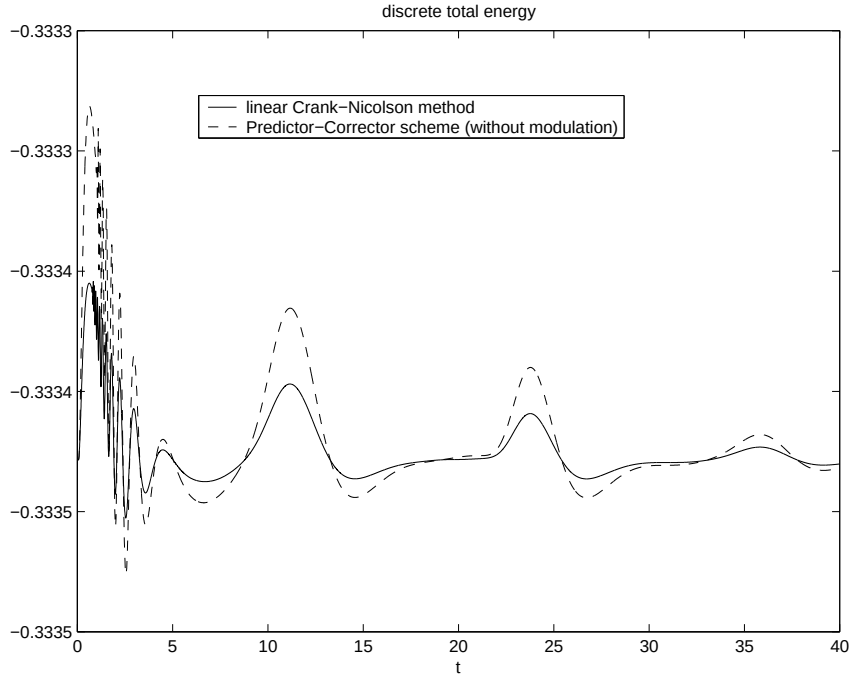

Fig. 5. Time evolution of the discrete total energy up to $T = 40$.

parameter ω is computed (cf. (28)) by

$$\omega_0 = -\frac{\Delta r}{2\Delta t^3} \frac{\sum_{j=1}^{J} \frac{\phi_j^{(n,2)} - \phi_j^{(n,1)}}{j} \left(\left| u_j^{(n,2)} \right|^2 - \left| u_j^{(n)} \right|^2 \right)}{\sum_{j=0}^{J-1} \mathrm{Im} \left\{ \bar{u}_j^{(n,2)} u_{j+1}^{(n,2)} \right\} \left(g_{j+1} - g_j \right)}.$$

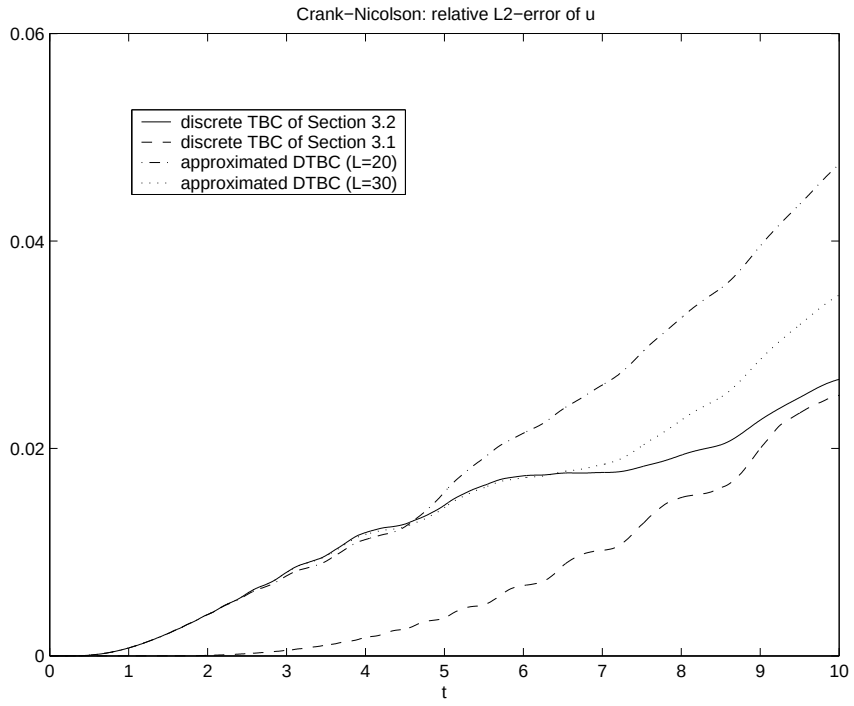

Fig. 6. Relative L^2-norm of the error in $u(r,t)$ for the linear Crank–Nicolson scheme.

However, in our numerical calculations this initial guess was already quite good ($R^{(n)}(\omega_0) \approx 10^{-7}$ – 10^{-9}) and therefore we used these values throughout our example and worked without the Newton iteration. It turned out that the choice of g_j has a negligible effect on the value of $R^{(n)}(\omega_0)$.

Finally, we want to investigate the induced error from using the different proposed boundary conditions. Again we use the linear Crank-Nicolson scheme and the predictor–corrector scheme with the modulation strategy (using $g(r) = 1/(1+r)$) on the computational interval $[0, 10]$. We computed a reference solution $u_{ref}^{(n)}$ on the enlarged domain $[0, 20]$ by the predictor–corrector method with the approximated new TBC ($L = 30$). In Fig. 6 and Fig. 7 we compare the relative L^2-norm of the error ($\|u^{(n)} - u_{ref}^{(n)}\|_2 / \|u^I\|_2$) for the different (approximated) discrete TBCs for the range from 0 to $T = 10$ (i.e. 1000 time steps). It turned out that the error for the predictor–corrector method is smaller than for the Crank–Nicolson scheme. Moreover, the error for the approximated DTBC with $L = 30$ is quite close to the one for the exact new DTBC (66). The error curves using the DTBC of §3.1 are identical for both schemes.

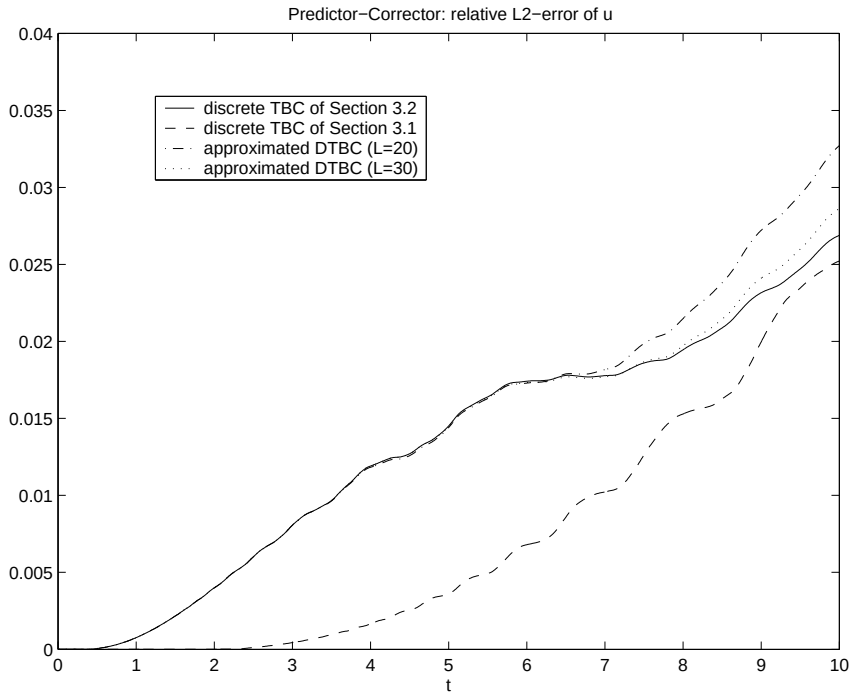

Fig. 7. Relative L^2-norm of the error in $u(r,t)$ for the predictor–corrector scheme.

Conclusions

We have proposed a variety of strategies to derive an approximation to the discrete TBC for an energy and mass conserving discretization of the Schrödinger equation with a Newton–type potential term in the exterior domain. Especially when investigating the existence of so–called *breathing mode* solutions (changing size oscillatory wave functions) it is of great importance to obtain an energy preserving method [23] (since the existence of these periodic solutions is a consequence of a minimizing variational principle with constraints, involving the energy). Therefore we will analyze in a forthcoming paper [10] the existence of so–called *discrete breathers solutions*. However, the last results in Fig. 6 and Fig. 7 indicates that the discrete TBCs shall be improved in a future work to take into account the coupling of the predictor and corrector step and the nonlinear modulation step. It seems to be necessary to take into account the asymptotic behaviour of the potential $\phi(r,t)$ for $r \to \infty$ when constructing the DTBC for u and the boundary condition at $r = R$ for ϕ.

Acknowledgement

The first author would like to acknowledge fruitful discussions with Christian Ringhofer, Enrique Ruíz Arriola and Juan Soler during his stay in Granada.

References

[1] A. Arnold, *Numerically Absorbing Boundary Conditions for Quantum Evolution Equations*, VLSI Design **6** (1998), 313–319.

[2] A. Arnold, M. Ehrhardt and I. Sofronov, *Discrete transparent boundary conditions for the Schrödinger equation: Fast calculation, approximation, and stability*, Comm. Math. Sci. **1** (2003), 501–556

[3] E. Bécache, F. Collino, M. Kern and P. Joly, *Higher order numerical schemes for the paraxial wave equation*, Mathematical Methods in Geophysical Imaging III, 1995.

[4] N. Ben Abdallah and O. Pinaud, *A mathematical model for the transient evolution of a resonant tunneling diode*, C. R. Math. Acad. Sci. Paris, **334** (2002), 283–288.

[5] N. Ben Abdallah, F. Méhats and O. Pinaud, *On an open transient Schrödinger–Poisson system*, HYKE Preprint 2004–084.

[6] A. Bultheel and M. Van Barel, *Linear algebra, rational approximation and orthogonal polynomials*, Studies in Computational Mathematics 6, North–Holland, 1997.

[7] F. Castella, *L^2-solutions to the Schrödinger–Poisson system: existence, uniqueness, time behaviour and smoothing effects*, Math. Mod. Meth. Appl. Sci. **7** (1997), 1051–1083.

[8] M. Ehrhardt, *Discrete Artificial Boundary Conditions*, Ph.D. Thesis, Technische Universität Berlin, 2001.

[9] M. Ehrhardt and A. Arnold, *Discrete Transparent Boundary Conditions for the Schrödinger Equation*, Riv. Mat. Univ. Parma **6** (2001), 57–108.

[10] M. Ehrhardt, E. Ruíz Arriola and J. Soler, *Existence of Discrete Breathers of the Schrödinger–Poisson System*, in preparation.

[11] E. Hairer and G. Wanner, *Solving ordinary differential equations II: Stiff and differential-algebraic problems*, Springer Series in Computational Mathematics 14, 2nd rev. ed., Springer–Verlag, 1996.

[12] R. Illner, P.F. Zweifel and H. Lange, *Global existence, uniqueness and asymptotic behaviour of solutions of the Wigner-Poisson and Schrödinger–Poisson systems*, Math. Meth. Appl. Sci. **17** (1994), 349–376.

[13] W.J. Lentz, *Generating Bessel Functions in Mie Scattering Calculations Using Continued Fractions*, Appl. Opt. **15** (1976), 668–671.

[14] J.H. Luscombe, A.M. Bouchard and M. Luban, *Electron confinement in quantum nanostructures: self–consistent Poisson–Schrödinger theory*, Phys. Rev. B **46** (1992), 10262–10268.

[15] W. Magnus, F. Oberhettinger and R.P. Soni, *Formulas and theorems for the special functions of mathematical physics*, 3rd ed., Springer-Verlag, 1966.

[16] P. Markowich, C. Ringhofer and C. Schmeiser, *Semiconductor equations*, Springer-Verlag, 1990.

[17] R.E. Mickens, *Asymptotic properties of solutions to discrete Coulomb equations*, Comput. Math. Appl. **36** (1998), 285–289.

[18] I.M. Moroz, R. Penrose and P. Tod, *Spherically–symmetric solutions of the Schrödinger–Newton equations*, Class. Quantum Grav. **15** (1998), 2733–2742.

[19] G. Reinisch, J. de Freitas Pacheo and P. Valiron, *Schrödinger–Poisson model for very–high–pressure cold helium*, Phys. Rev. A **63** (2001), 042505.

[20] C. Ringhofer and J. Soler, *Discrete Schrödinger–Poisson Systems preserving Energy and Mass*, Appl. Math. Lett. **13** (2000), 27–32.

[21] C. Ringhofer, *private communication.*

[22] E. Ruíz Arriola and J. Soler, *Asymptotic behaviour for the 3-D Schrödinger–Poisson system in the attractive case with positive energy*, Appl. Math. Lett. **12** (1999), 1–6.

[23] E. Ruíz Arriola and J. Soler, *A Variational Approach to the Schrödinger–Poisson System: Asymptotic Behaviour, Breathers, and Stability*, J. Stat. Phys. **103** (2001), 1069–1106.

[24] P. Tod and I.M. Moroz, *An analytical approach to the Schrödinger–Newton equations*, Nonlinearity **12** (1999), 201–216.

[25] R. Wong and H. Li, *Asymptotic expansions for second–order linear difference equations*, J. Comput. Appl. Math. **41** (1992), 65–94.

[26] A. Zisowsky, *Discrete Transparent Boundary Conditions for Systems of Evolution Equations*, Ph.D. Thesis, Technische Universität Berlin, 2003.